Effect of Liquid Metal Embrittlement on Mechanical Behavior of Advanced High-Strength Steel Spot Welds at Ambient and Low Temperatures




Authors

Kayla M. Molnar (top row, left) formerly of Colorado School of Mines, Golden, Colo., USA

Matthew L.S. Zappulla (top row, right) formerly of Colorado School of Mines, Golden, Colo., USA

John G. Speer (bottom row, left) John Henry Moore Distinguished Professor, Metallurgical and Materials Engineering, and director, Advanced Steel Processing and Products Research Center, Colorado School of Mines, Golden, Colo., USA jspeer@mines.edu

Kip O. Findley (bottom row, right) associate professor, Metallurgical and Materials Engineering, Colorado School of Mines, Golden, Colo., USA kfindley@mines.edu

Along with research aimed at understanding and improving liquid metal embrittlement (LME) resistance, the effects of LME cracks on mechanical performance should also be considered. Literature studies of tensile-shear and cross-tension tests with LME cracks did not indicate significant property degradation due to cracks smaller than 300 µm at room temperature. In the present work, the quasi-static strength of spot-welded specimens from a galvanized advanced high-strength steel was tested using tensile-shear and cross-tension with weld crack lengths near 480 µm. Each configuration was tested at room temperature and temperatures as low as –10°C. The peak load decreased with decreasing temperature for both test configurations, but there was no correlation of peak load with crack size or location. The failure modes of the cross-tension tests were consistent between test temperatures. However, tensile-shear tests showed predominantly button pullout failure at low temperatures and interfacial failure at room temperature. Finite element models were also developed for a 2D tensile-shear configuration to provide insight on critical crack geometries that affect performance. The highest stress near the crack tip exists for crack angles of approximately 60° with respect to the surface sheet surface, and stresses increase with increasing crack length. However, these stresses near the crack tip are significantly smaller than those at the weld edge; therefore, the models predict that LME cracks would have no influence on the tensile-shear failure mode.

This paper is the recipient of the 2020 AIST Jerry Silver Award. For more information about AIST awards, visit AIST.org.

New targets set for fuel efficiency and crash performance in the automotive industry have led to new developments in advanced high-strength steels (AHSS). Zn-coated AHSS have exhibited susceptibility to liquid metal embrittlement (LME) during spot welding. Automobiles contain between 2,000 and 5,000 spot welds; therefore, the integrity of spot welds is important.[1]

Many studies focus on the elimination of LME, but fewer studies have been performed to evaluate the influence of LME cracks on mechanical properties. Previous work has shown there is no degradation in cross-tension, tensile-shear and fatigue properties when Type B LME cracks are smaller than 300 µm.[2,3] A schematic cross-section of a spot weld shows an example of Type B cracking in Fig. 1 as well as other crack types. Significant changes in peak load, absorbed energy and fatigue cycles to failure are only observed when cracks are larger than 600 µm.[2,3] Further, the influence of temperature on mechanical behavior of specimens with LME is important to consider for lower-temperature service conditions of vehicles, and has not previously been evaluated.

For an LME crack to be detrimental to the load-bearing capacity of a spot weld, the stresses driving crack propagation must be greater than the stress for button pullout or interfacial fracture.[4] Comparing stress states around the weld edge and crack front is both experimentally and numerically challenging due to the complex three-dimensional geometry of LME cracks. As there are no existing analytical solutions

This article is available online at AIST.org for 30 days following publication.

Figure 1

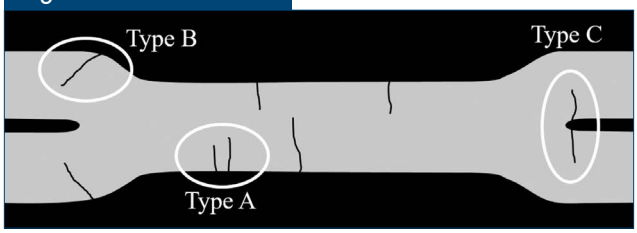

Possible types and locations of liquid metal embrittlement (LME) cracking in spot welded Zn-coated steel.

for stresses around spot weld cracks, finite element analysis (FEA) modeling should be an attractive method for analyzing critical crack geometries.

Experimental Procedure

Experimental Material — A galvanized AHSS with susceptibility to LME cracking was employed for the mechanical testing study. The steel is 1.5 mm thick with a tensile yield strength, ultimate tensile strength, and total elongation of 770 MPa, 1,090 MPa, and 20%, respectively. Spot welds for each testing configuration were produced with the intention of creating Type B LME cracks. Welding was performed with 8-mm ISO Type B electrodes with an electrode force of 1,100 lbs. and weld current of 9.7 kA. The weld time was 26 cycles, and the hold time was 10 cycles on a 60 Hz spot welder.

Crack Characterization — One tensile-shear and one cross-tension sample were analyzed using a Zeiss Xradia Versa 3D x-ray microscope to study the full 3D geometry of the LME cracks. Since all welds were produced with the same weld schedule, the cracks observed with the micro CT scan were considered representative of all welds provided. The remaining test samples were analyzed using red dye penetrant to determine the location and circumferential length of the Type B cracks as seen from the surface, which is referred to in this work as "arc angle." For example, the average weld diameter was 7.9 ±0.3 mm, so the circumferential length of a crack with a 90° arc angle is 6.2 mm. All crack dimensions from the x-ray CT microscope and red dye testing were measured using ImageJ software.

Mechanical Testing — Static strength testing of both specimen configurations was performed on a servo-hydraulic axial test frame. For both tests, a cross-head speed of 0.394 inch/minute (10 mm/minute) was used to determine the peak load to fracture. Samples of each configuration were tested at room temperature or at low temperature using an EXAIR® compressed air adjustable spot cooler with dual-point hose nozzles. For the tensile-shear samples, the nozzles were aligned with the spot weld, as shown in Fig. 2a. The temperature at the center of the weld was approximately –10°C and increased by 3°C at 6 mm away from the center. For cross-tension testing, the spot cooler nozzles were inserted into the testing configuration, as shown in Fig. 2b. The nozzles were further

Figure 2

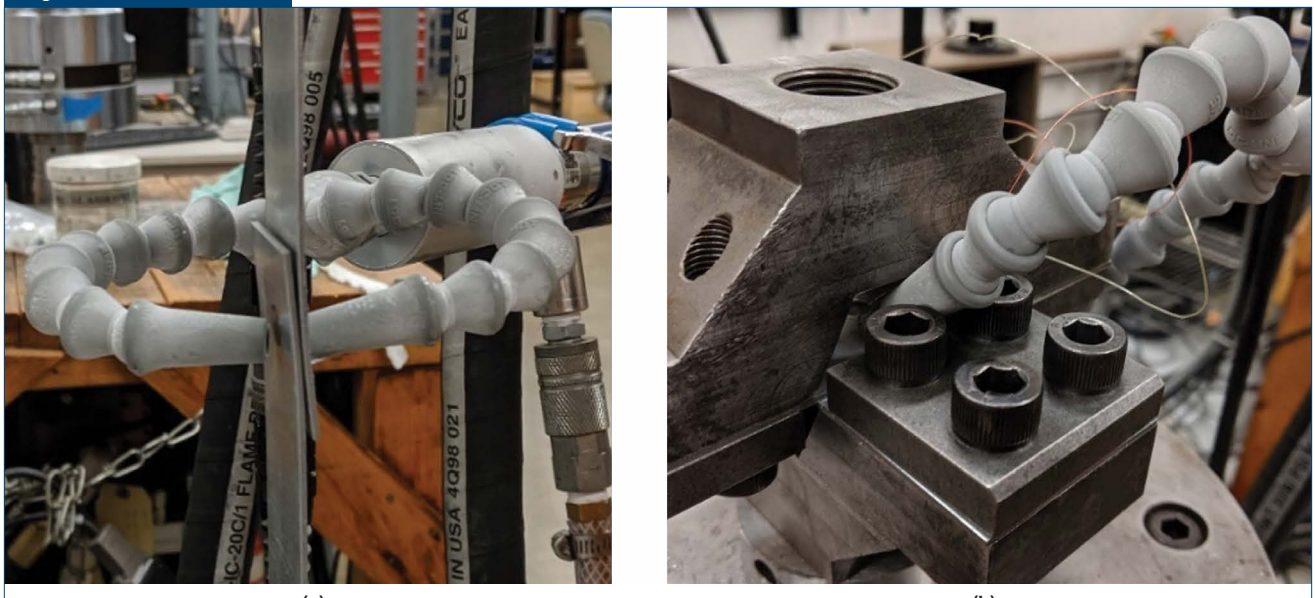

(a) (b)

Spot cooler setup for tensile-shear (a) and cross-tension testing (b).

Figure 3

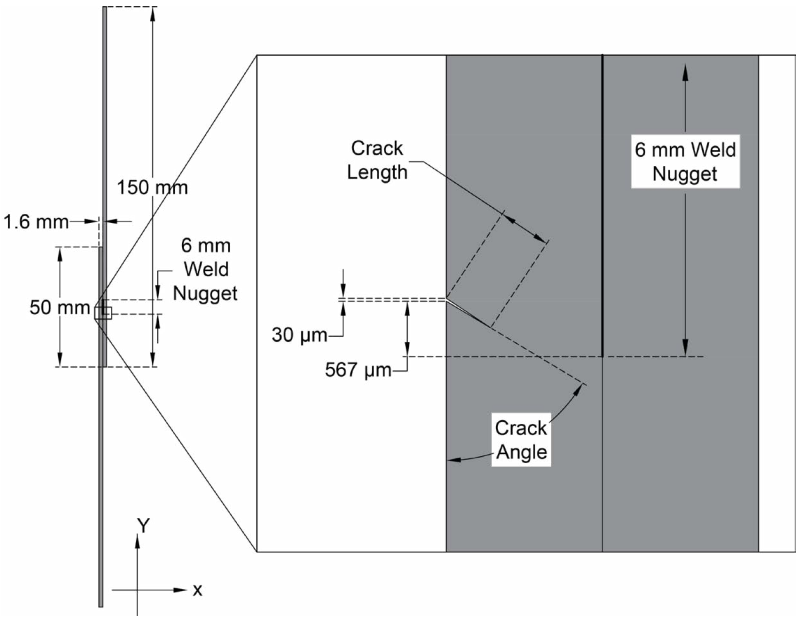

Schematic of the geometry of a 2D tensile-shear test and crack geometry used for finite element modeling.

Finite Element Modeling Methodology

A finite element model was developed using Abaqus/Standard to replicate the behavior of a 2D standard tensile-shear test.[5] A Young's modulus of 2.04 GPa was used, which is typical for carbon steel alloys. The material model is linear-elastic isotropic. The model uses the geometry shown schematically in Fig. 3, with a tie constraint used to represent the weld. A 2-mm displacement was imposed on the ends of the specimen to match the displacement achieved in previous AHSS spot weld tensile shear studies.[2] The specimen and crack dimensions are shown in Fig. 3. The crack opening on the surface, 30 µm, and distance from the edge of the weld nugget, 567 µm, were also derived from a paper by Choi et al.[2] The crack angle and length were varied in the parametric study. The crack angle was varied between 5° and 90° for a fixed crack length of 295 µm. Crack length was varied between 25 and 825 µm, to encompass the range of crack lengths found in previous studies of AHSS, with a fixed crack angle of 60°.[2] A mesh convergence study was performed, and an element size of 0.125 mm was chosen for the global mesh with a more refined mesh around the crack tip.

from the weld due to the geometry of the test fixtures, so the temperature at the center of the weld nugget was higher than the tensile-shear tests and averaged 1.2°C with a variance of ±4°C at a distance 6 mm away; the temperature depended on proximity to the spot cooler nozzle since blows on the top and bottom of the sample from one side each. The spot cooler was turned on five minutes prior to the beginning of each test to achieve a steady-state temperature distribution.

Figure 4

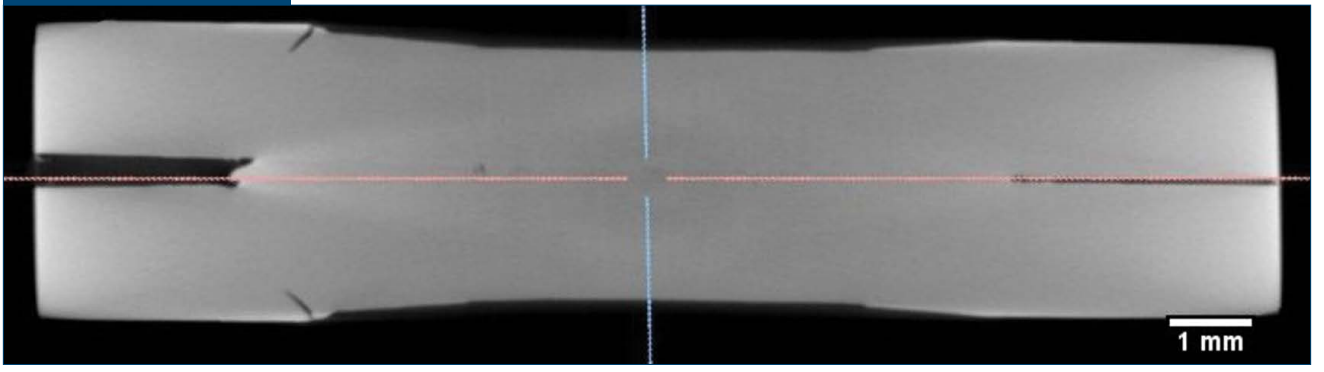

Cross-section image of a representative spot weld, imaged using the Zeiss Xradia Versa 3D x-ray microscope.

Figure 5

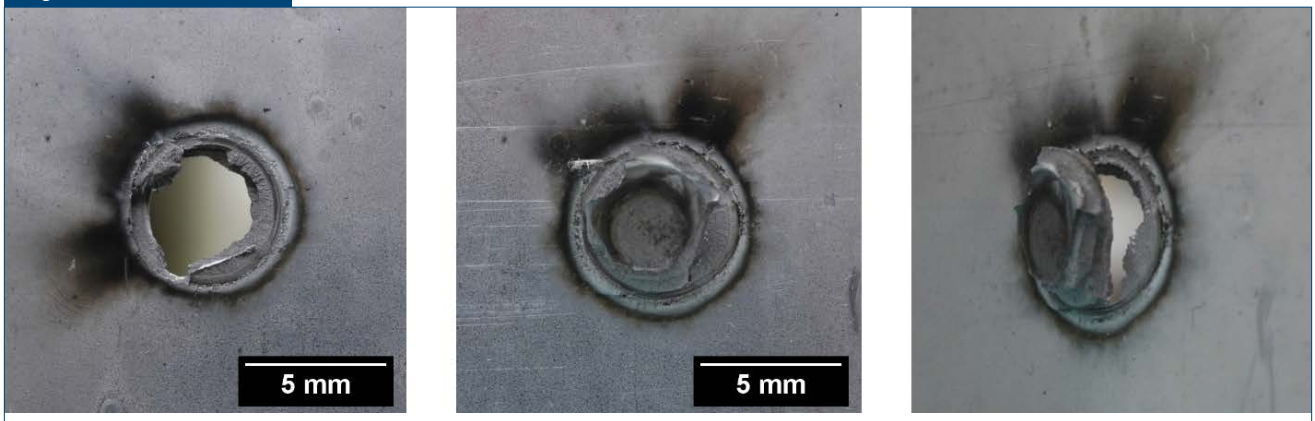

Room temperature cross-tension weld failure showing (a) sheet with weld nugget removal and partial interfacial fracture, (b,c) opposite sheet showing button pullout failure.

Results and Discussion

Crack Characterization — A representative cross-section of a spot weld obtained from the x-ray CT scan is shown in Fig. 4. The 3D scan revealed that the average representative crack angle with respect to the sample surface is 40°, and the maximum crack length is 480 µm. The LME cracks are also symmetrical on both sheets of material. The arc angle for the representative spot weld was 78°, while the average arc angle for all other spot-welded specimens was 70°. The location of the crack around the weld nugget varied between specimens.

Cross-Tension Testing — The average peak load was 4.67 kN with a standard deviation of 0.11 kN for the low temperature specimens and was 5.23 kN with a standard deviation of 0.38 kN for the room temperature samples. Overall, there was a 10.7% decrease in peak load at low temperature. For both test temperatures, the failure mode was a combination of partial interfacial failure and button pullout, as shown in the fractographs in Fig. 5.

The arc angles of the specimens tested ranged from 44° to 90°, but at low temperatures the peak load had no correlation with arc angle. Similarly, at room temperature, the difference in peak load did not correlate to differences in the crack arc angle or crack location. At both temperatures, failure mode was consistent and also did not correspond with crack geometry or location.

Tensile-Shear Testing — The tensile shear test results were classified into two groups. Four tests exhibited significantly lower peak loads at both room and low temperatures with an average of 21.3 kN and standard deviation of 2.30 kN. All of these welds had significant expulsion compared to welds from the other group, as shown in Fig. 6. Crack lengths and locations do not correlate to the area of expulsion. In the specimens with no expulsion, the peak loads were 29.62 kN with a standard deviation of 1.09 kN for low temperature and 33.17 kN with a standard deviation of 3.19 kN for room temperature. The average peak load of tests without expulsion decreased by 10.7% at low temperature. Although both cross-tension and tensile-shear decreased in peak load by the same amount, temperatures for tensile-shear were more than 10° colder.

For all low-temperature tests, the failure mode was either button pullout or double button pullout, where the weld nugget was removed from both sheets of material. At room temperature, the failure mode was predominantly interfacial or partial interfacial. Interfacial failures are traditionally associated with lower loads and a lower fracture toughness than button pullout failures. However, in this study, there was

Figure 6

Photographs of failed tensile-shear welds with no expulsion (a) and expulsion (b).

Figure 7

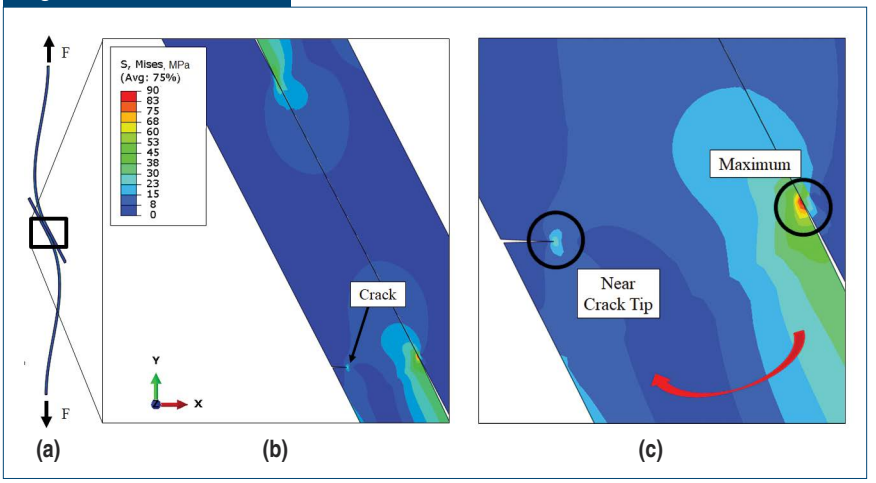

2D tensile-shear sample with crack after deformation (a), closer detail at weld nugget (b), and the location of maximum stress at weld edge and near the crack tip with an arrow showing the rotation of the bottom plate when the load is applied (c).

Figure 8

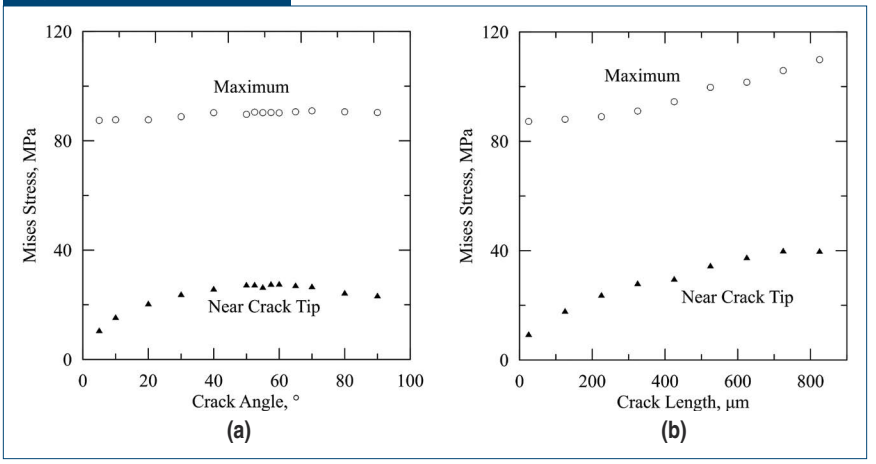

Maximum von Mises stress in the model, which is located at the edge of the weld nugget, and von Mises stress near the crack tip versus the crack angle at a fixed crack length of 295 µm (a) and the crack length at a fixed crack angle of 60° (b).

interfacial fracture at high loads and higher temperatures, i.e., where fracture toughness is presumably higher.[1,6,7] Chao illustrated that button pullout failure is directly related to the shear strength of the heat-affected zone (HAZ), and therefore low temperatures may decrease this shear strength.[1] Again, there was no correlation between the peak load and crack size or location.

Finite Element Modeling — The simulated deformed tensile shear specimen model is shown in Fig. 7; additionally, the von Mises stress contours are plotted in Figs. 7b and 7c. For each configuration in the parametric study, the maximum von Mises stress was determined in addition to the von Mises stress near the crack tip. The von Mises stress is utilized because it is an equivalent stress, so it is independent of the choice of axis, which is important in this study since the principal axes at the crack front and spot weld are not the same. Additionally, spot weld cracks may be subject to mode I, II and III opening stresses. While the dominant opening modes have not been determined yet, the von Mises stress is related to all three modes or mixed mode loading. The maximum stress was always located at the edge of the weld nugget tie constraint, as indicated in Fig. 7c, rather than near the crack tip.

The results showing the von Mises stress as a function of crack angle are presented in Fig. 8a. The von Mises stress near the crack tip peaks around 60°. The frequency of crack angles from various published studies of Type B LME cracks are graphed and compared to the von Mises stresses near the crack tip in Fig. 9.[2,3,8–12] The majority of cracks in literature occur at angles around 40°–55°, where the von Mises stress at the crack tip is the highest. However, recall that the maximum stresses near the weld nugget are significantly higher than the stress near the crack tip for each geometry. The maximum stresses at the weld nugget are also significantly higher for the full range of crack lengths modeled, as shown in Fig. 8b. For the crack length study, an angle of 60° was chosen to model the worst-case scenario of the crack. With increasing crack length, the stress at the crack tip increases but is still less than half of the maximum stress near the weld nugget. The maximum stress also increases with increasing crack length, particularly at crack lengths greater than 300–400 µm. By increasing the crack length, the distance between the crack tip and edge of the weld nugget decreases. A smaller distance, i.e., a larger crack, allows for more rotation of the bottom plate, which is likely the cause of increasing maximum stress at the edge of the weld nugget. This rotation, indicated in Fig. 7c, also closes and shears the crack opening. While the maximum stress

Figure 9

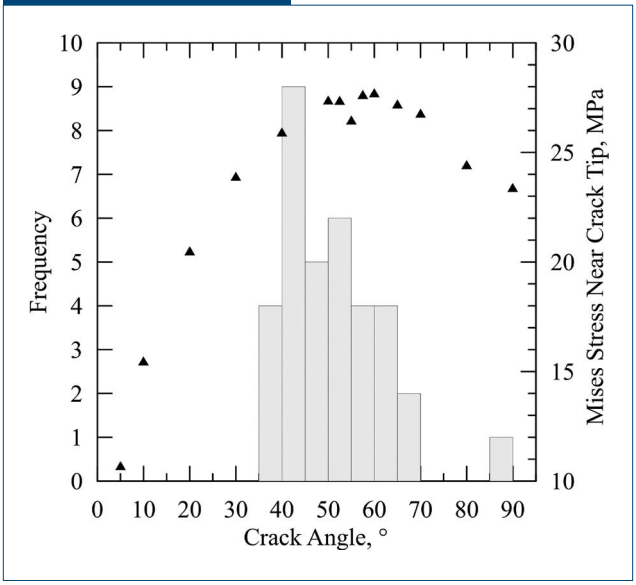

von Mises stress near the crack tip (triangles) compared to frequency of crack angle (bars) taken from various published Type B LME cracks.[2,3,8–12]

near the weld nugget increases at large crack lengths, the applied load is consistent with that applied for the smaller crack lengths. Thus, failure may occur sooner at large crack lengths, resulting in a lower peak load.

In work by Choi et al. and Benlatreche et al., there was no degradation in properties when Type B LME cracks were present in the tensile-shear configuration compared to samples with no cracks;[2,3] these findings are contrary to the results of the FE model in this work. However, the trend shown by the models is for a specific orientation of the crack with respect to the applied load; furthermore, the crack location in the model is associated with the highest stress intensity at the crack as well as the entire configuration, as shown by Zhang.[4] Experimentally, the crack location varied on each sample, and thus, the effects of the crack may not be significant, which could explain why this trend is not commonly observed. Additionally, since the maximum stress is located at the weld edge and the stress near the crack tip is small compared to the maximum stress, the model results suggest there should be little influence from the crack on the failure mode of the weld.

Summary

Mechanical testing of cross-tension and tensile-shear configurations show that spot weld performance is not degraded by crack size or location. With low-temperature testing, decreases in peak load were found for both configurations, as well as a change in failure mode for tensile-shear loading. FE modeling of the tensile shear configuration showed that the stresses near the weld nugget are higher than near the crack tip for the range of crack angles and lengths evaluated, indicating no effect of the crack on failure mode. However, crack length increases the maximum stress near the weld edge increases, indicating that the specimen may fail sooner and therefore decrease the peak load.

Acknowledgments

The authors acknowledge the support of the Advanced Steel Processing and Products Research Center, a National Science Foundation Industry/University Cooperative Research Center at the Colorado School of Mines.

References

1. Y.J. Chao, "Failure Mode of Spot Welds: Interfacial Versus Pullout," *Science and Technology of Welding and Joining,* Vol. 8, No. 2, 2003, pp. 133–137.
2. D.Y. Choi et al., "Liquid Metal Embrittlement of Resistance Spot Welded 1180 TRIP Steel — Effects of Crack Geometry on Weld Mechanical Performance," *MS&T17,* 2017, pp. 454–462.
3. Y. Benlatreche et al., "Spot-Weld Integrity of Zn-Coated 3rd Gen. Advanced High-Strength Steels in Presence of LME," *International Automotive Body Congress,* 2017, pp. 1–8.
4. S. Zhang, "Stress Intensities at Spot Welds," *Int. Journal of Fracture,* Vol. 88, No. 2, 1997, pp. 167–185.
5. ABAQUS 6.13 Theory Manual, DS Simulia Corp., Providence, R.I., USA, 2013.
6. D.J. Radakovic and M. Tumuluru, "Predicting Resistance Spot Weld Failure Modes in Shear Tension Tests of Advanced High-Strength Automotive Steels," *Welding Journal,* Vol. 87, 2008, pp. 96s–105s.
7. R.O. Ritchie et al., "On the Relationship Between Critical Tensile Stress and Fracture Toughness in Mild Steel," *Journal of the Mechanics and Physics of Solids,* Vol. 21, No. 6, 1973, pp. 395–410.
8. J. Barthelmie et al., "Liquid Metal Embrittlement in Resistance Spot Welding and Hot Tensile Tests of Surface-Refined TWIP Steels," *18th Chemnitz Seminar on Materials Engineering,* 2016, pp. 1–8.
9. G. Jung, "Zn-Assisted Liquid Metal Embrittlement of High-Mn Austenitic Steels," Ph.D. thesis, Graduate Institute of Ferrous Technology, 2015.
10. E.M. Van Der Aa et al., "Resistance Spot Weldability of 3rd Generation Advanced High-Strength Steels for Automotive Applications," *Steels in Cars and Trucks Conference,* 2017.
11. D. Choi et al., "Parametric Study for Liquid Metal Embrittlement in Resistance Spot Welds of Galvanized TRIP Steel," *Sheet Metal Welding Conference XVIII,* 2018, pp. 1–9.
12. Z. Ling, M. Wang and L. Kong, *Transactions on Intelligent Welding Manufacturing,* Springer, Singapore, 2018, pp. 25–42. ✦

MS&T MATERIALS SCIENCE & TECHNOLOGY This paper was presented at Materials Science & Technology (MS&T) 2019, Portland, Ore., USA, and published in the Conference Proceedings.